

Lithospheric Buoyancy and Continental Intraplate Stresses

MARY LOU ZOBACK AND WALTER D. MOONEY¹

Earthquake Hazards Team, U.S. Geological Survey, MS 977, 345 Middlefield Road, Menlo Park, California 94025

Abstract

Lithospheric buoyancy, the product of lithospheric density and thickness, is an important physical property that influences both the long-term stability of continents and their state of stress. We have determined lithospheric buoyancy by applying the simple isostatic model of Lachenbruch and Morgan (1990). We determine the crustal portion of lithospheric buoyancy using the USGS global database of more than 1700 crustal structure determinations (Mooney et al., 2002), which demonstrates that a simple relationship between crustal thickness and surface elevation does not exist. In fact, major regions of the crust at or near sea level (0–200 m elevation) have crustal thicknesses that vary between 25 and 55 km. Predicted elevations due to the crustal component of buoyancy in the model exceed observed elevations in nearly all cases (97% of the data), consistent with the existence of a cool lithospheric mantle lid that is denser than the asthenosphere on which it floats. The difference between the observed and predicted crustal elevation is assumed to be equal to the decrease in elevation produced by the negative buoyancy of the mantle lid. Mantle lid thickness was first estimated from the mantle buoyancy and a mean lid density computed using a basal crust temperature determined from extrapolation of surface heat flow, assuming a linear thermal gradient in the mantle lid. The resulting values of total lithosphere thickness are in good agreement with thicknesses estimated from seismic data, except beneath cratonic regions where they are only 40–60% of the typical estimates (200–350 km) derived from seismic data. This inconsistency is compatible with petrologic data and tomography and geoid analyses that have suggested that cratonic mantle lids are ~1% less dense than mantle lids elsewhere. By lowering the thermally determined mean mantle lid density in cratons by 1%, our model reproduces the observed 200–350+ km cratonic lithospheric thickness.

We then computed gravitational potential energy by taking a vertical integral over the computed lithosphere density. Our computed values suggest that the thick roots beneath cratons lead to strong negative potential energy differences relative to surrounding regions, and hence exert compressive stresses superimposed on the intraplate stresses derived from plate boundary forces. Forces related to this lithosphere structure thus may explain the dominance of reverse-faulting earthquakes in cratons. Areas of high elevation and a thin mantle lid (e.g., western U.S. Basin and Range, East African rift, and Baikal rift) are predicted to be in extension, consistent with the observed stress regime in these areas.

Introduction

THE CONCEPT OF ISOSTATIC EQUILIBRIUM in the Earth can be dated to the middle of the 19th century (Airy, 1855; Pratt, 1855), and was the consequence of modeling the deflection of geodetic plumb-lines in the vicinity of the Himalayan Mountains. The term “isostasy” was introduced by Dutton (1882) to describe “the floatation of the crust upon a liquid or highly plastic substratum.” The Airy model of compensation invokes a layer of constant density and varying thickness to explain differences in elevation. The Pratt model was based on a constant thick-

ness layer of laterally varying density. Support for the Airy model came from early crustal structure studies that indicated that most high mountain ranges have a thick root/crust. Extensive modern seismic refraction data indicate that elements of both models are valid—i.e., the crust has laterally varying density and thickness. Watts (2001) has presented a comprehensive review of the development of the concept of isostasy.

With the advent of plate tectonics theory, the rigid outer shell of the Earth, broken into tectonic plates, was defined as the lithosphere. The lithosphere, which includes both the crust and an attached mantle lid, was envisioned as floating on a warmer, fluid-like asthenosphere. A simple thermal model involving cooling and thickening of the

¹Email addresses: zoback@usgs.gov and mooney@usgs.gov, respectively.

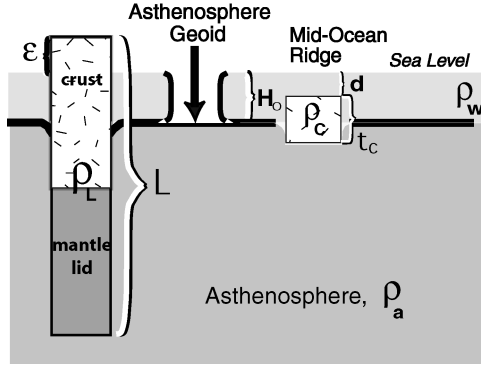


FIG. 1. Mass columns depicting the lithosphere buoyancy model described in the text, after Lachenbruch and Morgan (1990). Columns are assumed to “float” on an asthenosphere of density ρ_a . On the left is a general lithospheric column of elevation ϵ , thickness L , and average density ρ_L and consisting of a crust and mantle lid component. The right-hand column is a mid-ocean ridge, where ocean crust is assumed to rest directly on asthenosphere. This column is taken as a reference column, used to calculate the constant, H_o (km), the height of the asthenosphere geoid (the height the asthenosphere would rise to without an overlying lithosphere; Turcotte et al., 1977). Definitions: ρ_w , ρ_c , d , and t_c are, respectively, the average density of seawater, the density of crust of a mid-ocean ridge, the depth of mid-ocean ridges, and the thickness of oceanic crust (see Table 1 for representative values).

mantle lid of oceanic lithosphere successfully explains subsidence of the sea floor as it moves away from mid-ocean ridges (Parsons and Sclater, 1977; Sclater et al., 1980). This model works well because the oceanic crustal portion of the lithosphere, once formed, is very uniform in both density and thickness. Numerous workers have suggested a similar buoyancy model can be applied to explain the elevation of continental lithosphere (Crough and Thompson, 1976; Haxby and Turcotte, 1978; Davies, 1979; Fleitout and Froidevaux, 1982; LeStunff and Ricard, 1995), taking into account thermo-tectonic age as well as variations in crustal density and thickness.

Lachenbruch et al. (1985) and Lachenbruch and Morgan (1990) proposed a lithosphere buoyancy model to explain surface elevation in continental areas, and demonstrated the applicability of such a model based on province-wide averages and estimates of crust and upper mantle (lid) thickness and density. The purpose of this paper is to apply the model of Lachenbruch and Morgan (1990) using a detailed global-crustal-structure database, and combine this with a simple thermal model of the mantle lid in order to determine continental lithospheric thickness and density. We then use the depth integral of the density distribution within the lithosphere to compute potential energy differences relative to a standard reference column. Forces arising from the potential energy differences are

then compared to the state of stress in intraplate continental regions. We find that the cold, dense mantle lid exerts a negative buoyancy and hence compressive stress on the overlying crust, in accord with the dominance of strike-slip and reverse faulting within continental interiors.

Elevation as a Function of Lithosphere Buoyancy

In the lithosphere buoyancy model of Lachenbruch and Morgan (1990), a lithosphere of mean density ρ_L is assumed to float on an asthenosphere with a constant density of ρ_a (Fig. 1). These authors showed that:

$$\epsilon = \left[\frac{(\rho_a - \rho_L) \times L}{\rho_a} \right] - H_o \quad \epsilon \geq 0, \quad (1)$$

where ϵ is elevation above sea level, L is the thickness of the lithosphere, and H_o is the buoyant height of sea level relative to the hypothetical free surface of the asthenosphere—that is, the “asthenosphere geoid” of Turcotte et al. (1977). For the case of lithosphere submerged beneath seawater of density ρ_w , the elevation is given by:

$$\epsilon = \frac{\rho_a}{(\rho_a - \rho_w)} \left(\frac{(\rho_a - \rho_L)}{\rho_a} L - H_o \right) \quad (2a)$$

TABLE 1: Calculated Values for H_0 Based on Physical Properties of Mid-Ocean Ridge Crests

Crustal thickness, km	Average crustal density, kg/m^3	Asthenosphere density, kg/m^3	Seawater density, kg/m^3	Ridge elevation, kg/m^3	References	Calculated H_0 , km
6.50	2,877	3,300	1,030	2.30	Weiland and MacDonald, 1976	2.415
5.95	2,694	3,300	1,030	2.85	Stevenson and Hildenbrand, 1996	3.053
6.00	2,700	3,300	1,030	3.00	Madsen et al., 1984	3.154
7.00	2,875	3,300	1,000	2.70	Doin et al., 1996	2.567
7.00	2,875	3,200	1,000	2.70	Doin et al., 1996	2.783

or:

$$\varepsilon = \frac{(\rho_a - \rho_L)}{(\rho_a - \rho_w)} L - H_o \quad \varepsilon < 0. \quad (2b)$$

Lachenbruch and Morgan (1990) calibrated their buoyancy model using a mid-ocean ridge as a reference density column, assuming that, at the ridge crest, oceanic crust rests directly on the asthenosphere (i.e., there is no mantle lid). In this case the elevation of the ridge crest and of the density and thickness of the oceanic crust can be substituted into equation (2) to determine the constant H_o , the buoyant height of sea level relative to the free surface of the asthenosphere. Table 1 summarizes values for these parameters obtained from various bathymetry, gravity, geoid, and seismic studies at mid-ocean ridges. We use the mean of the values given in Table 1 as the best estimate for the constant H_o :

$$H_o = 2.78 \pm 0.35 \text{ km}. \quad (3)$$

Elevation produced by lithospheric buoyancy can be broken down into crustal (H_c) and mantle lid (H_m) components. If we include the constant H_o in the crustal buoyancy elevation, then the equations for these two components are:

$$H_c = \frac{1}{\rho_a} (\rho_a - \rho_c) \times L_c - 2.78 \pm 0.35 \text{ (km)} \quad (4)$$

$$H_m = \frac{1}{\rho_a} (\rho_a - \rho_m) \times L_m \text{ (km)}, \quad (5)$$

where ρ_c is the average crustal density, L_c is the crustal thickness, ρ_m is the density of the mantle lid, and L_m is the thickness of mantle lid. The elevation contribution due to crustal buoyancy is proportional to the thickness and average density of the crust. This buoyancy can be estimated in a straightforward manner if reliable data are available for crustal structure.

Computing Crustal Buoyancy from Crustal Structure Information

Crustal structure database

We use the USGS global database of the seismic structure of the crust to determine the thickness and average density of the crust. This database consists of over 1700 site-specific seismic P-wave velocity models interpreted from continental seismic refraction studies (Mooney et al., 1998, 2002). Each data point includes latitude, longitude, elevation, a one-dimensional model of the P-wave velocity structure, tectonic province, thermo-tectonic age (the age of the last significant deformational or magmatic event to affect a region), and heat flow. More than 90% of the crustal models were determined from seismic refraction surveys. The seismic velocity models are layered, and each layer consists of either a uniform velocity or a velocity gradient. The Moho was picked at the top of the layer where the P-wave velocity is greater than or equal to 7.6 km/sec (e.g., James and Steinhart, 1966). Elevations were determined from Etopo5 (National Geophysical Data Center, 1988) using a simple area average over a radius of 50 km around the data point. The tectonic

provinces and thermo-tectonic ages of the crust were determined from the summary of Goodwin (1996) and the Exxon Production Research Company (1985) tectonic map of the world.

Figure 2 shows the distribution of data used in this study on a base map of tectonic provinces. The bulk of the data (91%, 1584 out of 1739 determinations) was nearly evenly divided between three main tectonic regions: orogens (31%), extensional provinces (27%), and shields and platforms (15.7% and 18.7%, respectively). The remaining 9% of the data were measured in basins (4.7%), large igneous provinces that include flood basalt provinces and the East African rift (2.9%), and oceanic plateaus (1.3%). Measured continental crustal thickness ranges from 18 to 80 km, with more than 90% of the determinations in the range between 24 and 56 km.

Conversion of velocity information to density

There have been many proposals to quantify the relationship between seismic velocity and density. For this study we have relied on two principal ones. Following Mooney et al. (1998), we consider that portion of the crust with seismic velocities less than 4.5 km/s as sedimentary rock. For this portion of the crust, densities were determined using a widely accepted velocity-density relationship:

$$\rho = 1741(V_p^{0.23}), \quad (6)$$

where V_p is the P-wave velocity (km/sec) and ρ is the sedimentary rock density (kg/m^3) (Gardner et al., 1974). The density of a water layer, assumed to be seawater, was set at $\rho = 1050 \text{ kg/m}^3$.

Densities of non-sedimentary crustal rocks were determined using the linear velocity-density equations developed by Christensen and Mooney (1995) based on laboratory high-pressure measurements. For the crystalline crust, we have adopted the constants for the suite of measurements that exclude volcanic and mono-mineralic rocks. Densities for each layer in the velocity-depth model were computed using regression parameters applicable to the depth of the midpoint of the layer:

$$\rho = A + B(V_p), \quad (7)$$

where A and B are coefficients that vary as a function of depth (pressure) of the layer.

The table of regression coefficients from Christensen and Mooney (1995) is repeated here as Table 2 to correct two errors in their published tabulation (N. I. Christensen, 1998, pers. commun.). The A and

TABLE 2. Regression Coefficients for Velocity-Density Relationship in Crystalline Rocks¹

A	B	Applicable depth
540.6	360.1	0–15
444.1	375.4	16–25
381.2	388.0	26–35
333.4	398.8	36–45
287.8	409.4	>45

¹Corrected from Christensen and Mooney, 1995.

B values for depths >45 km they reported were incorrect, which resulted in a large overprediction of density for deep crustal depths.

Results—Crustal Buoyancy

Surface elevation is plotted as a function of crustal thickness in Figure 3. For the vast majority of the data (crustal thickness between 20–55 km) no clear relationship is apparent between elevation and crustal thickness. An Airy-type correlation between elevation and crustal thickness (i.e., thicker crust associated with higher elevation), exists only at the extreme values (crustal thickness >55 km or <20 km). In fact, large regions of continental crust at or near sea level (0–200 m elevation) have crustal thickness that range between ~25–55 km. The general lack of correlation between crustal thickness and elevation indicates that mantle buoyancy may be a significant contributor to surface elevation, a suggestion made by George Thompson in 1964 (Thompson and Talwani, 1964). These authors used gravity and seismic data from the western United States to show that regions of high elevation appeared to have thin crust underlain by a low-density (buoyant) uppermost mantle. Their general model of the Basin and Range crust and upper mantle structure was confirmed by later work (c.f., Thompson et al., 1989; Jones et al., 1996).

A comparison of average continental crustal density as a function of crustal thickness (Fig. 4) reveals a rather unexpected result: on average, mean crustal density increases with increasing crustal thickness, except for the very thickest crust sampled (crustal thickness = 55 km). This result runs counter to commonly assumed single values for average continen-

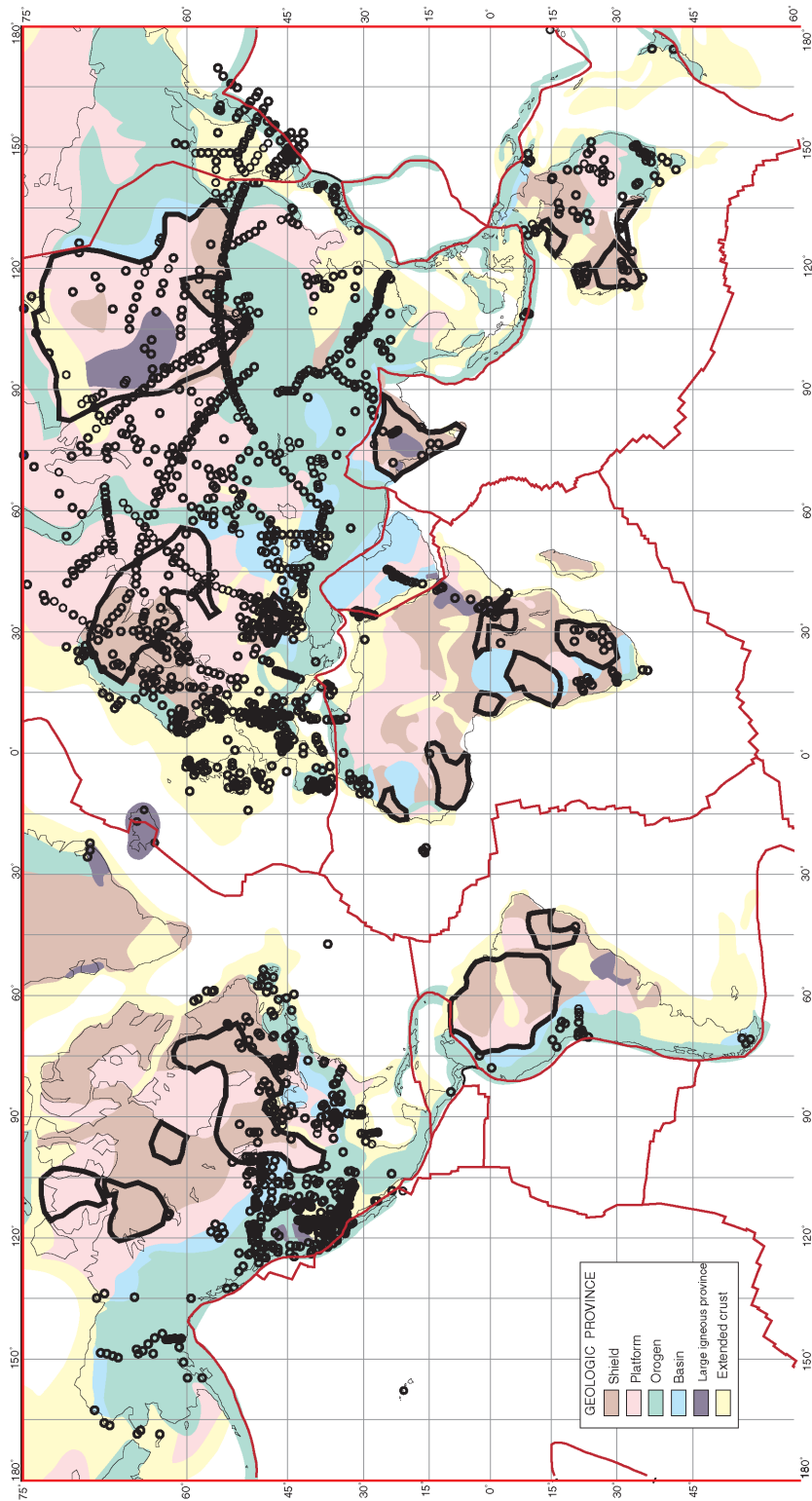


FIG. 2. Distribution of the 1,739 data points used from the global crustal structure database (Mooney et al., 1998; 2002) shown on a base of tectonic provinces after Goodwin (1996). Archean cratonic regions are outlined in heavy black lines.

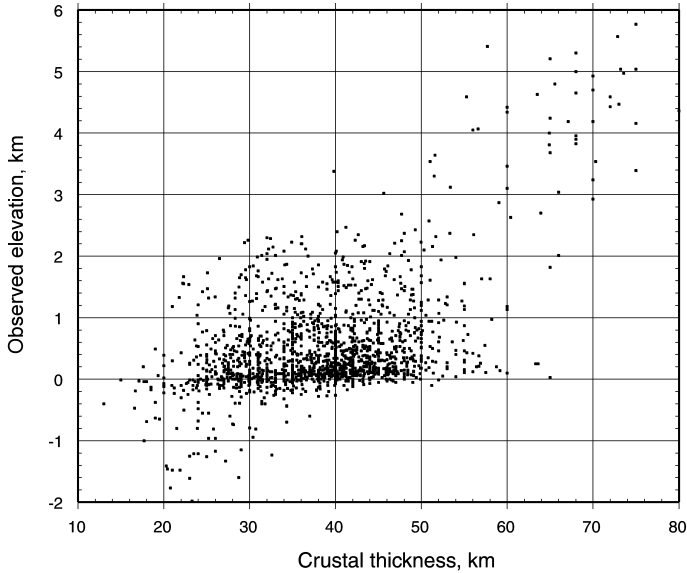


FIG. 3. Observed surface elevation versus crustal thickness from the Mooney et al. crustal structure database. Note that crust with a thickness of ca. 25–55 km show no systematic increase in elevation.

tal crustal density applied in many studies. The relationship shown in Figure 4 suggests on average a 6.5% difference in the 2764 kg/m^3 average density of 25 km thick crust, compared to a density of 2947 kg/m^3 for 50 km crust. The increase in crustal density as a function of increasing crustal thickness has important implications for the mechanism of crustal growth. It suggests that such growth is accomplished largely by: (1) preferential thickening of the lower crust, possibly by ductile flow; (2) mechanical thickening by overriding relatively dense oceanic or near oceanic crust/lithosphere; or (3) underplating and thickening of the lower crust by mafic intrusions. The breakdown of this relationship for the thickest crust ($> \sim 55 \text{ km}$) where average densities are comparatively low, probably indicates mechanical thickening of the upper crust in active orogens.

What role does the crust play in controlling surface elevation? Figure 3 indicates that crustal thickness is not a good predictor of surface elevation. Furthermore, Figure 4 indicates that thicker crust is also denser, which would tend to suppress an increase in elevation associated with increasing crustal thickness. Therefore, in this study, we assume that surface elevation is not related simply to crustal thickness but to lithosphere buoyancy—i.e., the product of thickness and average density of the entire lithosphere.

Using the seismic refraction information on crustal velocities and thickness, it is straightforward to apply equation (4) to predict the portion of surface elevation that is due to crustal buoyancy (assuming $\rho_a = 3300 \text{ kg/m}^3$, see Table 1). The results, shown in Figure 5, indicate that the predicted elevations from equation (4) are almost always (for 97% of the data) higher than the observed elevation, regardless of thermo-tectonic age or province type. A significant result is that, on average, the “crustal buoyancy”—predicted elevations in Figure 5 are $1.73 \pm 0.95 \text{ km}$ higher than the observed elevations. This implies that a dense lithospheric mantle lid is required to “pull” the crust down. Thus, the difference between the observed and predicted elevations in Figure 5 represents the mantle contribution to elevation in our lithosphere buoyancy model.

Computing Mantle Lid Thickness from Mantle Buoyancy

The $1.73 \pm 0.95 \text{ km}$ average difference between observed and predicted elevation from crustal buoyancy is taken as direct measure of H_m (elevation produced by mantle buoyancy) as given in equation (5). The negative values for mantle buoyancy elevation are consistent with the Lachenbruch and Morgan (1990) model in which the mantle lid and asthenos-

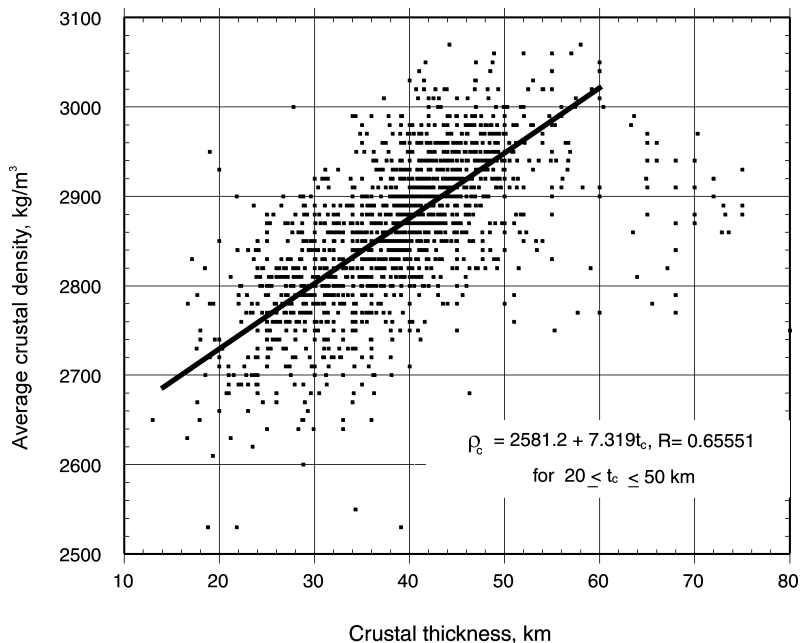


FIG. 4. Computed average crustal density versus crustal thickness. Crustal density increases for crust 20–50 km thick; for crust 50–80 km thick the average density is lower, and shows wide scatter and no clear trend.

phere are considered to be the same material, and the “negative” buoyancy of the lid results from its cooler temperatures.

Mantle buoyancy is proportional to the product of mantle lid thickness and density (equation 5). We can estimate mantle lid thickness from the mantle buoyancy elevation values needed to obtain the correct observed elevations, if we independently determine mantle lid density. Following Lachenbruch and Morgan (1990), we first assume a simple thermal model of the mantle lithosphere to determine mean mantle density from thermal expansion:

$$\rho_m = \rho_a[1 + \alpha(\Theta_a - \Theta_m)]. \quad (8)$$

The mantle lid geotherm is assumed to pass linearly from the base of the crust to the base of the lithosphere, so the mean mantle lid temperature, Θ_m , is simply the average of the crust base (Moho) temperature Θ_c and an assumed temperature for the base of the lithosphere, Θ_a , of 1350°C (c.f., Boyd and McCallister, 1976; Anderson, 1989). Although the temperature gradient in tectonically active areas is probably not strictly linear, the linear extrapolation is a reasonable approximation for the buoyancy

analysis (Lachenbruch and Morgan, 1990) in all but the youngest, hottest regions.

It is thus straightforward to calculate the mantle lid thickness L_m by combining equations (5) and (8):

$$L_m = \frac{-2H_m}{\alpha(\Theta_a - \Theta_c)}, \quad (9)$$

where α is the coefficient of thermal expansion, taken here as $3.5 \times 10^{-5} \text{K}^{-1}$ (Lachenbruch and Morgan, 1990). The negative sign in the above equation is due to the fact, as noted above, that the mantle buoyancy elevation, H_m , is negative, because the mantle lid is denser than the asthenosphere it displaces.

Heat-flow values were determined for each datapoint in the crustal-structure database using the compilation of Pollack et al. (1990, 1993) and updated with more recent studies (Artemieva and Mooney, 2001). The updated database of Pollock et al. (1993) was first interpolated and smoothed. Then, heat-flow values at seismic data points were extracted. This procedure is accurate where heat-flow data are available with a spacing of ~ 100 km

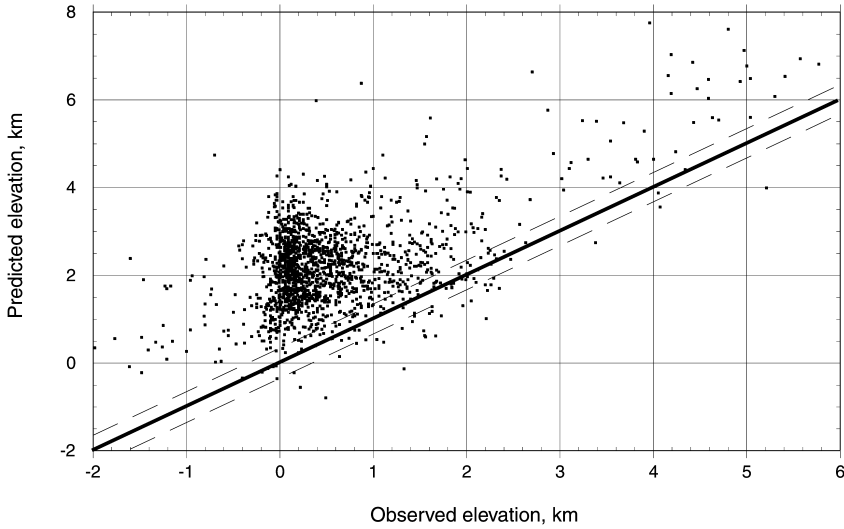


FIG. 5. Elevation predicted from crustal buoyancy (eq. 4) versus observed elevation. The solid line corresponds to the predicted elevation equal to observed elevation. The vast majority (97%) of the data plot above this line, indicating that the elevation predicted from crustal buoyancy generally exceeds the observed elevation. This implies that, on average, the subcrustal lithosphere exerts a negative buoyancy force on the crust to produce observed elevations. The dashed lines indicate the 350 m uncertainty in constant H_0 .

(such as for parts of North America and Europe) but can yield non-representative values where such data are sparser, and the closest measurement may come from a different tectonic regime. For this study, many anomalous, site-specific heat-flow values in the database were modified to represent province averages where these are well established (e.g., North America, Lachenbruch and Sass, 1977; Morgan and Gosnold, 1989; and Europe, Cermak and Bodri, 1995).

The temperatures at the base of the crust were computed for all points in the database by downward extrapolating surface heat flow after removing the upper-crustal radioactive contribution. If we assume a uniform thermal conductivity within the crust, k , the Moho temperature is obtained using the equation (Lachenbruch and Sass, 1978):

$$\Theta_c = \frac{1}{k} \left[(q - DA_0)L_c + D^2 A_0 (1 - e^{-L_c/D}) \right], \quad (10)$$

where q is surface heat flow, D is the “characteristic depth” for the vertical distribution of heat production, A_0 is the radioactive heat production, and L_c is, as before, crustal thickness. This equation is valid if heat transfer in the crust is predominantly by

steady-state conduction, which we assume for this global study, particularly inasmuch as province-average heat flows were generally used. Where the radioactive constants (D and A_0) are known for specific provinces, they were used in equation (10) (Morgan and Gosnold, 1989, for the continental U.S.; Jessop et al., 1984; Mareschal, 1991; and Pinet et al., 1991, for Canada; Oxburgh, 1981 for Scotland and Norway; Cermak, 1993 for much of Europe; and Balling, 1995 and Kukkonen, 1993 for the Baltic shield). Otherwise, we used standard continental values of $A_0 = 2 \mu\text{Wm}^{-3}$, $D = 10$ km, and $k = 2.5 \text{ Wm}^{-1}\text{K}^{-1}$ (Sass et al., 1981). In actively extending terrains where advection is important, this conductive approach will underestimate the Moho temperature (Lachenbruch and Sass, 1977, 1978), which could lead to an overestimate of lithospheric thickness.

Results—Lithospheric Thickness

Thermal model of the mantle lid

We sum the observed crustal thickness and the mantle lid thickness computed by applying the simple thermal buoyancy model described above to determine lithosphere thickness. A total of 1331 data points in the crustal structure database pro-

vided all the information needed to compute lithosphere thickness. The results are shown on the map of tectonic provinces in Figure 6A and the actual computed values of lithosphere thickness are given as a function of thermo-tectonic age in Figure 7. Most of the values of lithospheric thickness fall within the range of seismically and thermally determined thickness—i.e., between ~50 and 300 km. There is considerable scatter in all the computed lithosphere thicknesses, although the mean thickness values (indicated by the arrows) for all but the Archean data are similar, between ~150 and 180 km. In the next section we discuss uncertainties in this calculation. As the histogram plots in Figure 7 indicate, the thinnest values of lithosphere thickness generally correspond, as expected, to the tectonically youngest lithosphere (Mesozoic–Cenozoic age). In particular, thin lithosphere is predicted in young, actively extending regions such as the Basin and Range province of the western United States, the East African rift, and also in Western Europe (Fig. 6A). Anomalously thin lithosphere thickness values (~50–130 km) are also predicted for some Proterozoic data points (Fig. 7); these thin lithosphere values correspond to the relatively high densities computed for Proterozoic lids discussed below.

Close inspection of Figure 6a and the values in Figure 7 indicates that the thermal lid model also predicts relatively thin lithosphere (50–<180 km) for major portions of several Archean cratonic areas, including the Canadian and Baltic shields, where seismic studies have indicated thick, deep roots with lithosphere thickness of 200–350+ km (Grand, 1994; van der Lee and Nolet, 1997; van der Hilst et al., 1998; Simons et al., 1999; Ritsema and van Heijst, 2000). This discrepancy suggests that a simple thermal model for the mantle lid may not be appropriate for these regions. This conclusion was reached years ago through numerous seismic, heat-flow, geoid, and geochemical studies indicating a chemically distinct, relatively buoyant mantle lid beneath Archean cratons that may extend to depths of 400 km (Jordan, 1975, 1979, 1988; Boyd and McCallister, 1976; Boyd, 1989). These authors attribute the relatively low density of the Archean mantle to basalt depletion, associated with a high degree of melting of the uppermost mantle due to higher mantle temperatures during the Archean. The creation of a buoyant mantle lid has helped to stabilize these cores of Archean continental blocks (Jordan, 1975, 1978, 1981, 1988; Pollack, 1986).

Tectosphere model of the mantle lid

Doin et al. (1996) analyzed geoid anomalies related to lithospheric structure globally, and concluded that the lack of marked geoid lows over old cratons (with seismically determined thick mantle lids) implied a negative petrologic density anomaly of ~1%, in good agreement with the values inferred from kimberlite samples. Accordingly, we reduced our thermally determined densities by 1% for all data points of Archean age. The lid densities computed assuming the simple thermal model are shown in histograms in Figure 8 by thermo-tectonic age. The adjusted (reduced) densities for the Archean data points represent a distinct population indicated by the lighter shading.

The thermal lid densities we determined range between 3304 and 3367 kg/m³; these values are nearly identical to the 3310–3370 kg/m³ range of lid densities calculated by O'Reilly et al. (2001) using mean mineral compositions inferred from xenoliths. However, although our densities show a great deal of scatter and no apparent correlation with thermo-tectonic age, O'Reilly et al. (2001) concluded that the mean mantle lid density predicted from composition alone increases from the Archean to Phanerozoic. They found the most significant differences in composition and density between the Archean (3310±16 kg/m³) and Proterozoic (3340±20 kg/m³) mantle lids. The 1% density reduction we made for Archean mantle lid densities (lighter shading on Fig. 8) results in Archean densities somewhat higher than, but much closer to, the 3310±16 kg/m³ value they calculated. Our thermally computed mean lid densities for Proterozoic lithosphere are nearly all larger than O'Reilly et al.'s mean value of 3340±20 kg/m³, whereas the Paleozoic and Mesozoic–Cenozoic lid densities are generally less than the O'Reilly et al. mean Phanerozoic value of 3360±20 kg/m³. The large range of densities we compute for Mesozoic–Cenozoic mantle lid (Fig. 8) reflects the the limitations of the simple conductive geotherm assumed in these regions and thus the important role that heat and dynamics plays in determining what constitutes the lithosphere in these active terrains.

Figure 6B shows our final predicted lithosphere thicknesses, which are based on the thermal model of the mantle lid (thus, the same as Fig. 6A) except for the adjustment for compositional differences in the upper mantle beneath Archean terrains (outlined in black on both figures). The effect of the 1% reduction in the lid density in these regions is to

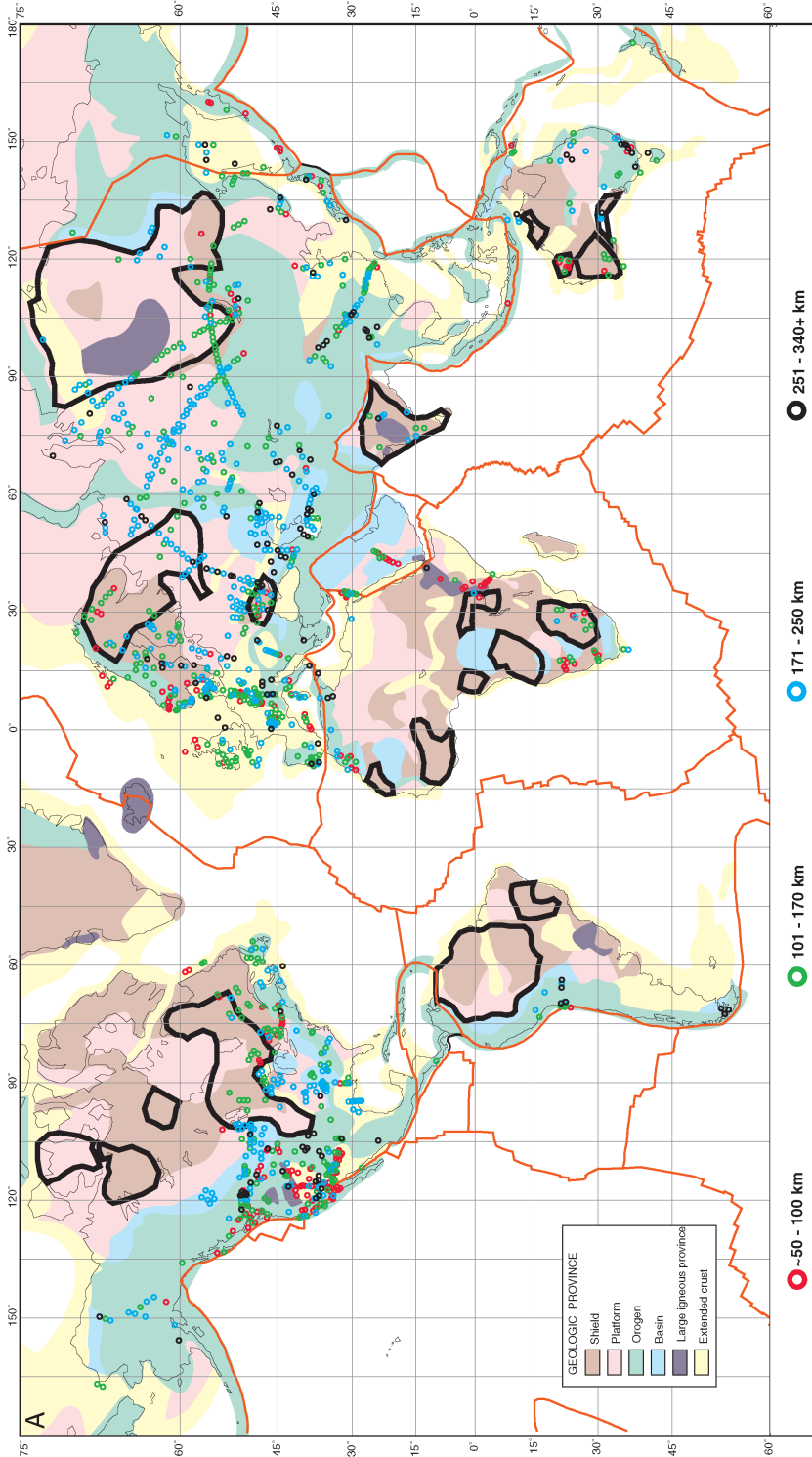


FIG. 6. A. Map of lithosphere thickness derived from the buoyancy model assuming a simple thermal model of the mantle lid. Lithospheric thickness is divided into four ranges (see key), between 50 and 340 km. This model does not take into consideration the lid density decrease within Archean cratonic regions (outlined in heavy black line) due to chemical depletion. B (facing page). Map of lithosphere thickness derived from the buoyancy model assuming a simple thermal model and with a 1% reduction in lid density beneath the Archean cratons (outlined in heavy black line). Lithospheric thickness is divided into four ranges (see key), between 50 and 340 km.

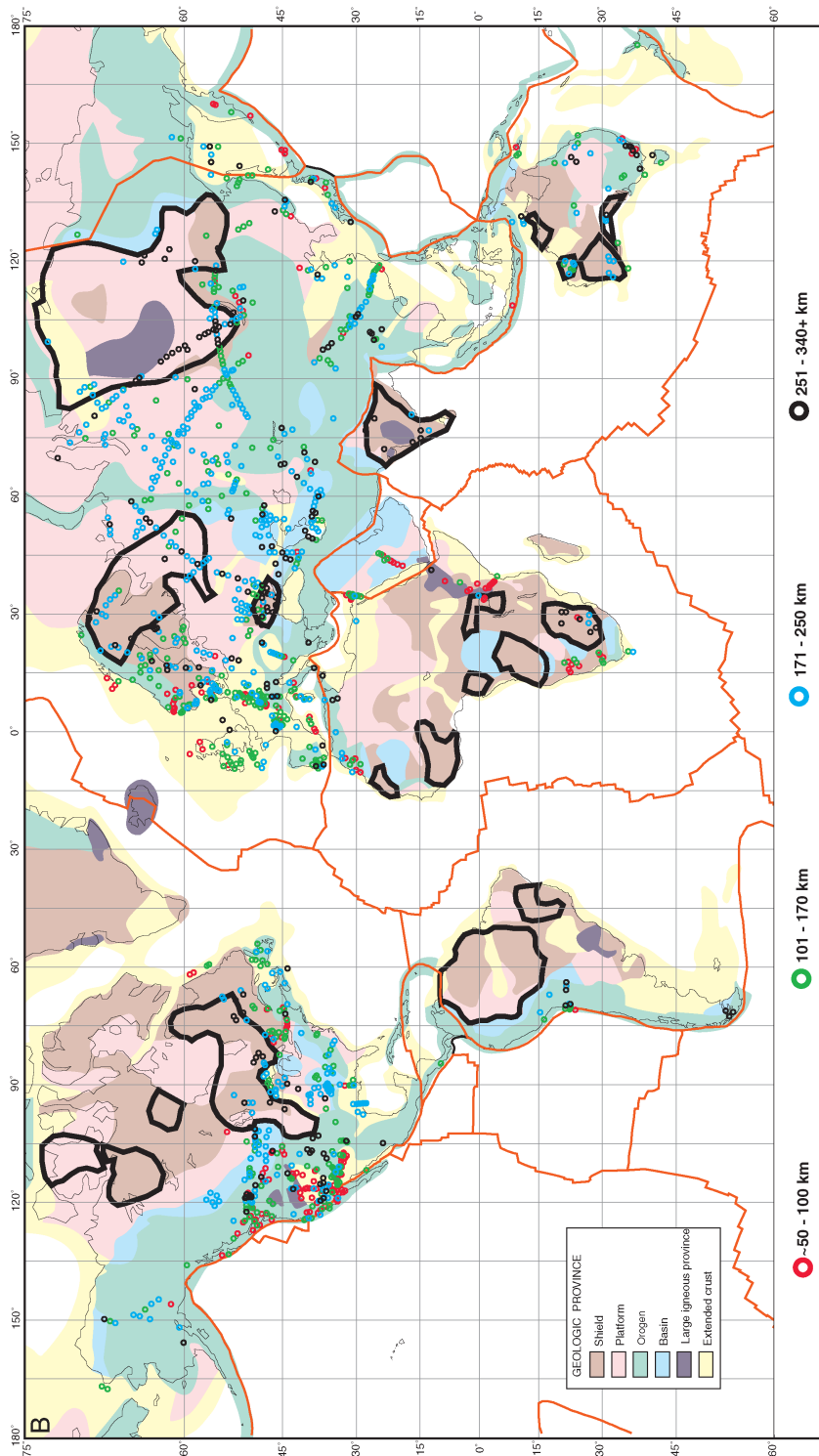


FIG. 6B.

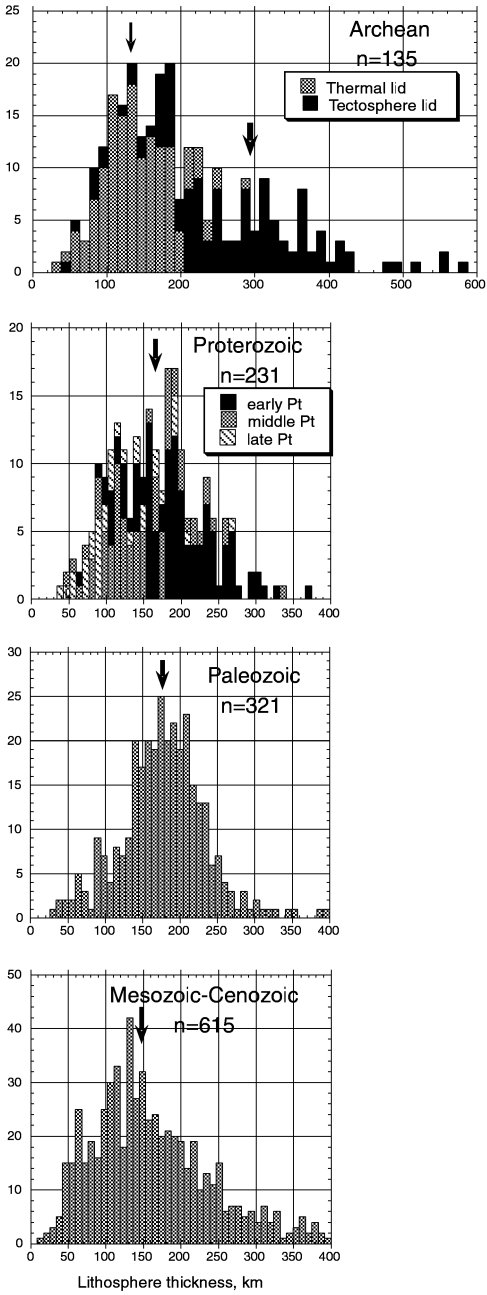


FIG. 7. Histograms of computed values of lithospheric thickness plotted as a function of thermo-tectonic age. Mean values for each age range indicated on each histogram by the arrows; n gives the number of determinations for each age range. For the Archean, lithosphere thicknesses from both the thermal and tectosphere models of the mantle lid are plotted; the mean values of these two distributions are indicated by the thin and thick arrows, respectively.

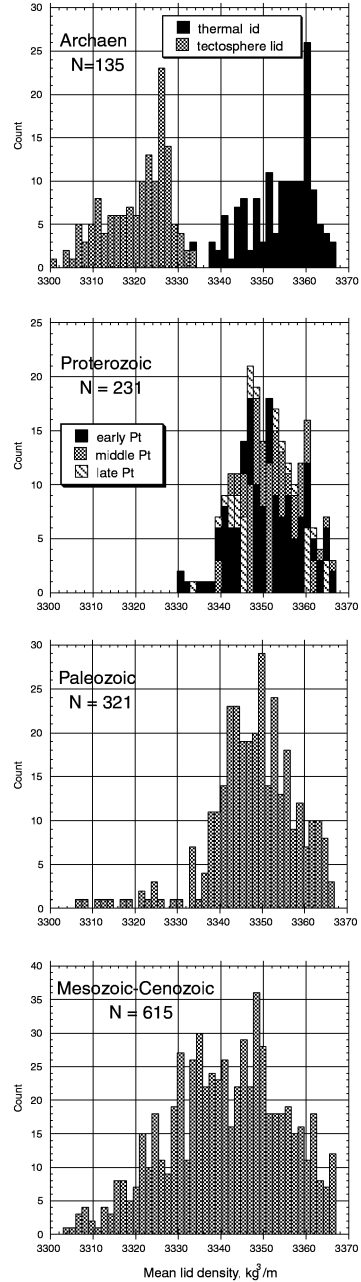


FIG. 8. Histograms of computed values of mantle lid densities as a function of thermotectonic age; n gives the number of determinations for each age range. Densities were determined assuming a linear mean mantle temperature (as described in the text). A petrologic density correction for Archean mantle lid results in reduced densities, as indicated by the shaded histogram.

increase lithosphere thicknesses to be more consistent with seismic results, which generally yield thicknesses of 200 km and greater (as discussed in the next section). The contrast in lithospheric thicknesses obtained from the thermal and tectosphere mantle lid models for the Archean data points is well illustrated by the histograms in Figure 7. The thermal model predicts anomalously thin Archean lithosphere thicknesses, generally in the range of 100–200 km, whereas, the tectosphere lid model predicts significantly greater thicknesses, generally in the range of 175–380 km.

The effect of the 1% lid density reduction has on lithosphere thickness is perhaps best demonstrated by example, for a representative crustal structure data point from the Canadian Shield. In an area where the measured crustal thickness is 38 km, the mean crustal density was determined to be 2940 kg/m³, yielding a predicted crustal buoyancy elevation of 1.43 km above sea level. The actual elevation is 350 m, thus the mantle buoyancy elevation component is -1.08 km. The thermal model for the density of the mantle lid (3351 kg/m³) resulted in a lid thickness of 71 km, and hence a total lithosphere thickness of 109 km, much shallower than the 200 km+ thickness indicated by seismic studies (Grand, 1994; van der Lee and Nolet, 1977). When the 1% petrologic density correction is made to the lid density, the density is reduced to 3320 kg/m³, and the resulting total lithosphere thickness is 248 km, much more consistent with the seismic results.

It is important to point out that in terms of the buoyancy calculation, the two models of the mantle lid are equivalent. However, as we will see in a later section, because the potential energy depends on the vertical integral of the mass distribution, there can be dramatic differences in the computed potential energy differences, depending on the vertical distribution of mass.

Comparison with seismological data on lithospheric thickness

It is of interest to compare our estimates of lithospheric thickness with those derived from seismology. For this comparison we use shear (S)-wave velocity models primarily obtained from the global inversion of seismic surface waves (Ritsema and Van Heijst, 2000). This choice is justified by the fact that surface-wave data provide better resolution of S-wave velocity in the upper mantle than body-wave data (Lay and Wallace, 1995). Also, since our buoyancy approach for estimating lithospheric thickness

was applied consistently and globally, we wanted to compare the results with a consistent global seismic analysis. We have adopted a conventional definition of the base of the continental lithosphere as the depth where the positive S-wave velocity anomaly decreases to a value of +1% (relative to the global mean). The uncertainty in this depth was estimated from the depth range spanned by +1.5% and +0.5% velocity anomalies (i.e., $1\% \pm 0.5\%$). We have selected 10 regions to make our comparison, 6 cratonic and 4 non-cratonic (Table 3). Seismic data from Ritsema and Van Heijst (2000) (Ls, Table 3) indicates that Archean cratonic lithosphere ranges in thickness from 205 to 300 km, with an average value of 240 km. In contrast, noncratonic lithosphere ranges in thickness from 50 to 200 km, with an average value of ~100 km. The comparison of seismic estimates with buoyancy-determined estimates (L_b^*) shows excellent agreement (most values agree within 10–15%). The largest discrepancy is for the early Paleozoic West Siberian Platform, where the buoyancy-estimated lithospheric thickness (185 km) for this noncratonic region appears to be more reasonable than the seismic value (245 km). In this case, it appears that the buoyancy estimate, which is based on point data, has higher resolution than the estimate from long-wavelength surface waves. Nevertheless, Table 3 indicates that buoyancy and seismic estimates of lithospheric thickness are highly compatible.

Discussion—Uncertainties in the Lithosphere Buoyancy Calculations

Before using the lithospheric density and thickness values to compute gravitational potential energy and evaluate its implications for continental stress state, it is useful to examine the multiple sources of uncertainty in the series of calculations presented above. The errors and uncertainties can be divided into three main categories: (1) model applicability—both the buoyancy model and the simple conductive thermal model for the mantle; (2) uncertainties in crustal thickness and velocities; (3) uncertainties in observed heat flow and radioactive heat constants that constrain mantle lid temperatures.

The buoyancy model used here assumes local isostasy over the scales of interest. Clearly, the flexural strength of the lithosphere limits the wavelength over which isostasy applies. In general, the assumption of “local isostasy” is probably valid only

TABLE 3. Comparison of Lithospheric Thickness Obtained from Buoyancy Calculations and Seismic Data¹

Region	Lat.	Long.	Number	L_b , km	L_{b^*} , km	L_s , km
Archean cratonic regions						
Aldan Shield	60°N	95°E	27	144 ± 23	285 ± 58	275 ± 35
Baltic Shield	66°N	35°E	16	140 ± 32	266 ± 80	255 ± 20
Superior Shield	50°N	95°W	20	118 ± 19	265 ± 62	235 ± 10
Kaapvaal craton	29°S	29°E	9	133 ± 43	300 ± 121	250–300 ²
W. Australia Shield	32°S	120°E	12	95 ± 19	172 ± 44	205 ± 10
Non-cratonic regions						
West Siberian Platform	60°N	75°E	37	185 ± 30		245 ± 20
E. Australia	35°S	140°E	20	235 ± 102		200 ± 25
W. Europe	50°N	8°E	31	124 ± 28		90 ± 30 ³
Basin and Range province, W. United States	40°N	114°E	15	70 ± 33		64 ± 20 ⁴

¹Two values are given for the buoyancy thickness; one assumes a thermal lid (L_b) the other assuming a thermal lid with a 1% lid density reduction for Archean cratons (L_{b^*}). Seismically determined lithosphere thicknesses (L_s) are from the global tomographic S-wave velocity model of Ritsema and Van Heijst (2000) except where more focused regional studies are available, as noted.

²James et al., 2001.

³Panza et al., 1980.

⁴Preistly and Brune, 1978.

at wavelengths greater than flexural thicknesses, which can vary from less than 10 km in hot, active provinces, to more than 100 km in older, colder lithosphere (McNutt et al., 1988; Watts, 2001). This fact implies that the lithosphere density structure obtained from the buoyancy model is best viewed in terms of region or province averages, not individual point values. It is also consistent with the observed elevations assigned to each data point, which represent elevations averaged over a 50-km radius.

Following Lachenbruch and Morgan, we used a simple linear conductive gradient to determine temperature and corresponding density in the mantle lid. A quasi-stationary thermal state is approached in a layer one to three conductive time constants τ after a rapid change in basal temperature or heat flux at its base, where $\tau = z^2/vA$; z is the layer thickness, and v = thermal diffusivity (Lachenbruch and Sass, 1978). The conductive time constant for an average lid thickness of 100–150 km is about 60–150 million years. We obtain this estimate from the definition of thermal diffusivity, $v = k/\rho c_p$, and using

the following values: $k = 4.0$ W/m²K in the upper mantle (Artemieva and Mooney, 2001), our average lid density of 3335 kg/m³, and $c_p = 1.0$ kJ/kgK (Fowler, 1990). Thus the steady-state assumption for the thermal regime in the mantle lid is probably justified for provinces that have been tectonically quiescent for the last several hundred million years (thermo-tectonic ages of Paleozoic or older, which represents about 55 percent of the data used to compute lithospheric thickness). Furthermore, the linear gradient we have assumed probably is also a reasonable approximation for many young provinces with thin mantle lids. Note that the conductive time constant for a 50 km lid is only 15 m.y.

The buoyancy model applied here relies on detailed knowledge of crustal structure, both layer thickness and velocity. In particular, it requires that the crustal thickness be well known, because the Moho is generally the largest density contrast within the lithosphere, typically 300–400 kg/m³. Fortunately, this parameter is generally one of the best determined from seismic refraction studies. For the

more recent (post-1980) high-quality seismic data, we estimate an average uncertainty of 5% in the crustal thickness values in the database. This uncertainty corresponds to ± 1.2 km and ± 2.5 km for a 25 and a 50 km thick crust, respectively. The effect of this uncertainty in crustal thickness on the calculation of lithospheric buoyancy can be evaluated by comparing the density contrast between: (1) the crust and the subcrustal lithosphere (Moho) versus (2) the mantle lid and the asthenosphere. As noted above, the average density contrast at the Moho is ~ 350 kg/m³, about an order of magnitude greater than the contrast at the bottom of the mantle lid. Thus, a 5% uncertainty in crustal thickness could give rise to an error in mantle lid thickness of 12 to 25 km (corresponding to a 25 and 50 km thick crust, respectively).

Average crustal density is obtained by converting the measured P-wave velocity structure to density. Modern (post-1980) measurements of crustal P-wave velocities have an average uncertainty of $\pm 3\%$ (Mooney, 1989). However, older studies with more widely spaced receivers have an uncertainty closer to $\pm 5\%$. The conversion of seismic velocity to density has an average uncertainty of ± 50 kg/m³, which generally coincides with a density uncertainty of about $\pm 2\%$ (Christensen and Mooney, 1995). Thus the overall uncertainty of the average crustal density is about ± 5 – 7% , similar to or perhaps slightly greater than the percentage uncertainty in crustal thickness. Uncertainties in average crustal density can produce uncertainties in the crustal buoyancy elevation (and hence uncertainties in lithospheric thickness) of 17–35 km for crust with thicknesses between 25 and 50 km. Thus, cumulatively, errors in crustal structure and computed densities could contribute up to ± 29 – 60 km of uncertainty in lithosphere thickness. However, the true range in uncertainties is probably significantly smaller because the crustal velocity and crustal thickness are inversely correlated—e.g., if the crustal velocity (hence density) used is high, then the resulting value of crustal thickness will be low.

Another significant source of uncertainty in the determination of mantle lid thickness is the mean density assumed for the lid. As indicated by the example calculation in the preceding section for an Archean shield, a thermally determined 1% reduction in the mean lid density can result in a threefold increase in lid thickness. Because the thermal effect on mean lid density is determined directly from the difference between the assumed temperatures at the

Moho and asthenosphere, our computed lid densities depend critically on the reliability of our heat flow/heat production values, and the applicability of the simple thermal conductive regimes assumed for both the crust and upper mantle. Where nearby heat-flow values were available and reasonably dense (roughly 35–40% of the database), province-average values were used to avoid local heat-flow perturbations, such as those due to hydrologic disturbances. Measured radioactive heat constants were available from regional studies for roughly 30% of the data. For the remainder of the points, representative continental constants were used to remove the radioactive contribution to heat flow.

The applicability of simple thermal conductive models was discussed above. These models will be poor approximations of the thermal regime for the youngest (thermotectonic age of less than ca. 15 million years) and hottest regions. However, the uncertainties in Moho temperature produce much smaller density variations than the 1% density reduction assumed due to depletion beneath Archaean cratons. A $\pm 50^\circ\text{C}$ uncertainty in the estimated temperature at the Moho can lead to an uncertainty in mean mantle lid density of only .01%. This same $\pm 50^\circ\text{C}$ uncertainty in Moho temperatures yields uncertainty in lid thickness ranging between $\pm 5.5\%$ and $\pm 10\%$ for Moho temperatures in the average range of 450°C to 850°C , respectively. For the average value of mantle buoyancy elevation found in this study, 1.73 ± 0.95 km, this $\pm 50^\circ$ uncertainty in Moho temperatures results in lid thickness uncertainties of ± 6 – 20 km for the average value and up to ± 30 km for the full range of mantle buoyancy elevation values. The largest uncertainty and scatter is to be expected in the thermally warmest areas, consistent with the wide range of computed lithosphere thickness values for the Mesozoic–Cenozoic datapoints in Figure 7.

The overall uncertainty of our calculations are reduced by virtue of having numerous measurements of crustal structure, uncertainties of which are expected to scatter around the true value without systematic bias. Thus, our calculated values of lithospheric thickness should also scatter around the “true” values, subject to the validity of our modeling assumptions. Based on the error analysis above, any individual lithospheric thickness determination may have an uncertainty of up to ± 40 – 60 km. Probably the best demonstration of the validity of the analysis used here is the fact that the vast majority of the computed lithosphere thicknesses (91%) fall

within the ~50–300 km range of seismically measured lithosphere thicknesses. Furthermore, because the buoyancy model restricts us to looking only at relatively long wavelength features (~100+ km), we feel our results can be used to represent province averages and regional differences in lithospheric structure between provinces.

Potential Energy Differences Due to Variations in Lithospheric Structure and Implications for Intraplate Stress

Lateral density variations in the lithosphere are associated with variations in lithospheric potential energy, which give rise to forces that can be an important source of intraplate stress (e.g., Frank, 1972; Artyushkov, 1973; Lister, 1975; Molnar and Tapponier, 1978; Houseman et al., 1981; Fleitout and Froidevaux, 1982, 1983). These studies show that elevated and thickened continental crust has a tendency to spread, creating extensional stresses within the elevated mass. In contrast, a thickened mantle lid, denser than the asthenosphere surrounding it, has negative buoyancy and leads to compressional stresses. The difference of the gravitational potential energy, ΔPE , of a lithospheric column relative to a reference lithosphere with which it is in isostatic balance (taken here as the asthenosphere geoid shown on Fig. 1 with no lithosphere or water above it) is given by:

$$\Delta PE = \int_{H_0}^L \rho_a g z dz - \int_{-\epsilon}^L \rho(z) g z dz, \quad (11)$$

where L is the depth of compensation (thickness of the lithosphere), H_0 is the elevation of the asthenospheric geoid (2.78 km below sea level; see Table 1), and ϵ is surface elevation (e.g., Fleitout and Froidevaux, 1982; Jones et al., 1996). The first term in equation (11) is the potential energy of the asthenospheric geoid reference column, the second term is the potential energy of the computed lithosphere density/thickness columns in this study. ΔPE represents an integrated vertical normal stress anomaly. Under the assumption of no boundary stresses except those induced by the reference column, ΔPE represents the integrated deviatoric stress (Jones et al., 1998). In this case, negative potential energy differences give rise to horizontal deviatoric compression, whereas positive potential energy differences indicate that the column is in a state of

horizontal deviatoric extension. Relative to the asthenosphere geoid, the mid-ocean ridge crust we used as the elevation reference has a positive (extensional) potential energy difference of 2.5×10^{12} N/m, roughly equivalent to the computed ridge-push force generated by thickening oceanic lithosphere as it moves away from the ridge and cools (e.g., Parsons and Richter, 1980; Dahlen, 1981). Absolute stress values are determined by the local gradient of the potential energy of the lithosphere. However, because our crustal structure data set does not represent a consistently and uniformly sampled grid, we have instead relied on potential energy differences (relative to the reference asthenosphere geoid) to indicate regional variations in deviatoric stress values.

We used the layered crustal density structure obtained from seismic refraction velocities and the thermally defined linearly decreasing density function in the upper mantle (eq. 8) to compute local potential energy differences according to equation (11). The density contrast of the mantle lid with the reference asthenospheric geoid column varies linearly from $2(\rho_m - \rho_a)$ at the top of the mantle lid to zero at the base of the lithosphere. Therefore, the potential energy differences computed are not strongly sensitive to the lowermost part of the lithosphere, and hence to the exact value of lithosphere thickness. However, distributing the same mass over a greater thickness of the mantle lid will increase the potential energy difference, which is proportional to (depth)². For example, in the previous section we showed for a typical point in the Canadian Shield that a 1% reduction in lid density resulted in an increase in predicted lid thickness from 78 to 210 km (corresponding to an increase in total lithospheric thickness from 109 to 249). Both lids have the same mass/cross-sectional area, but lowering the density contrast requires a thicker lid, resulting in a significantly more negative (compressional) potential energy difference, increasing from 2.24 to 3.98×10^{12} N/m.

Our computed potential energy differences are shown in Figure 9 as a function of observed elevation. For reference, we have also included the potential energy differences derived from crustal buoyancy alone. These values are uniformly positive, but the net potential energy differences for the entire lithosphere, including the mantle lid, show a spread of values from minor extension to predominantly compression compared to the reference asthenosphere geoid. Despite the scatter, several

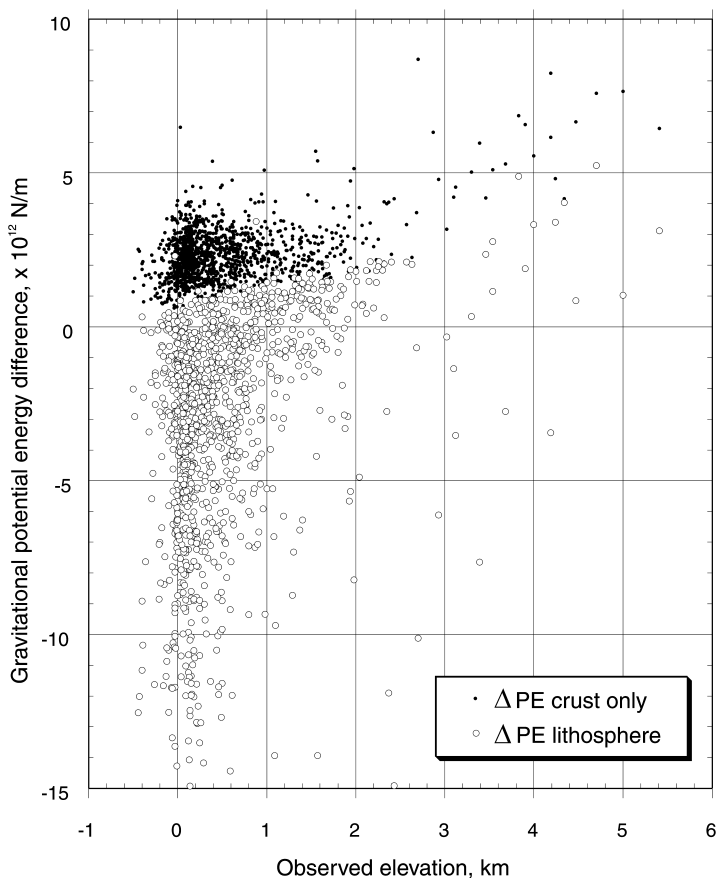


FIG. 9. Computed potential energy differences relative to the asthenosphere geoid (see text); values for the entire lithosphere are shown as open circles, values for the crust alone are indicated by small dots. The potential energy differences were computed from equation 11 using the lithosphere thickness and density model obtained from the buoyancy analysis. Negative values of ΔPE give rise to horizontal deviatoric compression, whereas positive ΔPE values indicate that the column is in a state of horizontal deviatoric extension. For reference, the mass column we used for mid-ocean ridges as the elevation reference has a positive potential energy difference (consistent with observed extension at the ridges) of 2.5×10^{12} N/m.

generalizations can be made. First, continental areas with average elevations above 1.5–1.75 km are nearly always predicted to be in a state of deviatoric extension. The higher the elevation, the greater the computed potential energy difference. In contrast, most low-lying continental regions (700 m and lower) have negative potential energy differences, and hence are predicted to be in a state of deviatoric compression. As noted above, the 1% density reduction in the Archean mantle lid produces thicker lithosphere and hence more negative values of potential energy differences, insofar as the lid mass is distributed deeper.

The general deviatoric state of stress predicted from lithosphere buoyancy is compared with observed stress regime data from the World Stress Map (Zoback, 1992) in Figure 10. The stress regime data plotted in Figure 10B are a subset of the World Stress Map database and represent only those data points with stress regime information, primarily earthquake focal mechanisms and geologic stress indicators. In Figure 10A we have selected a color scheme for representing the potential energy differences that should generally correlate with the stress regime: positive potential energy differences giving rise to deviatoric extensional stresses are shown in

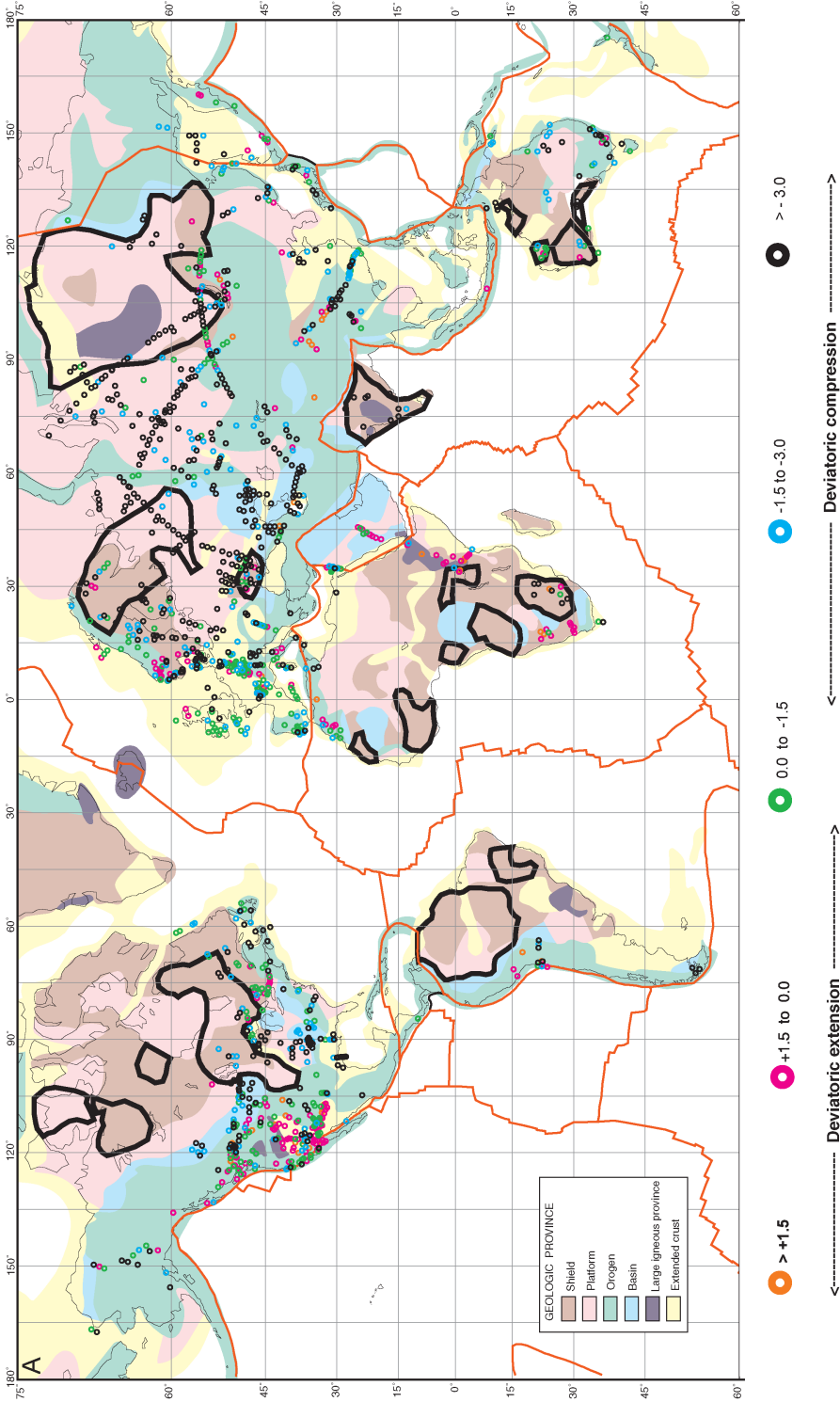


FIG. 10A. Caption on following page.

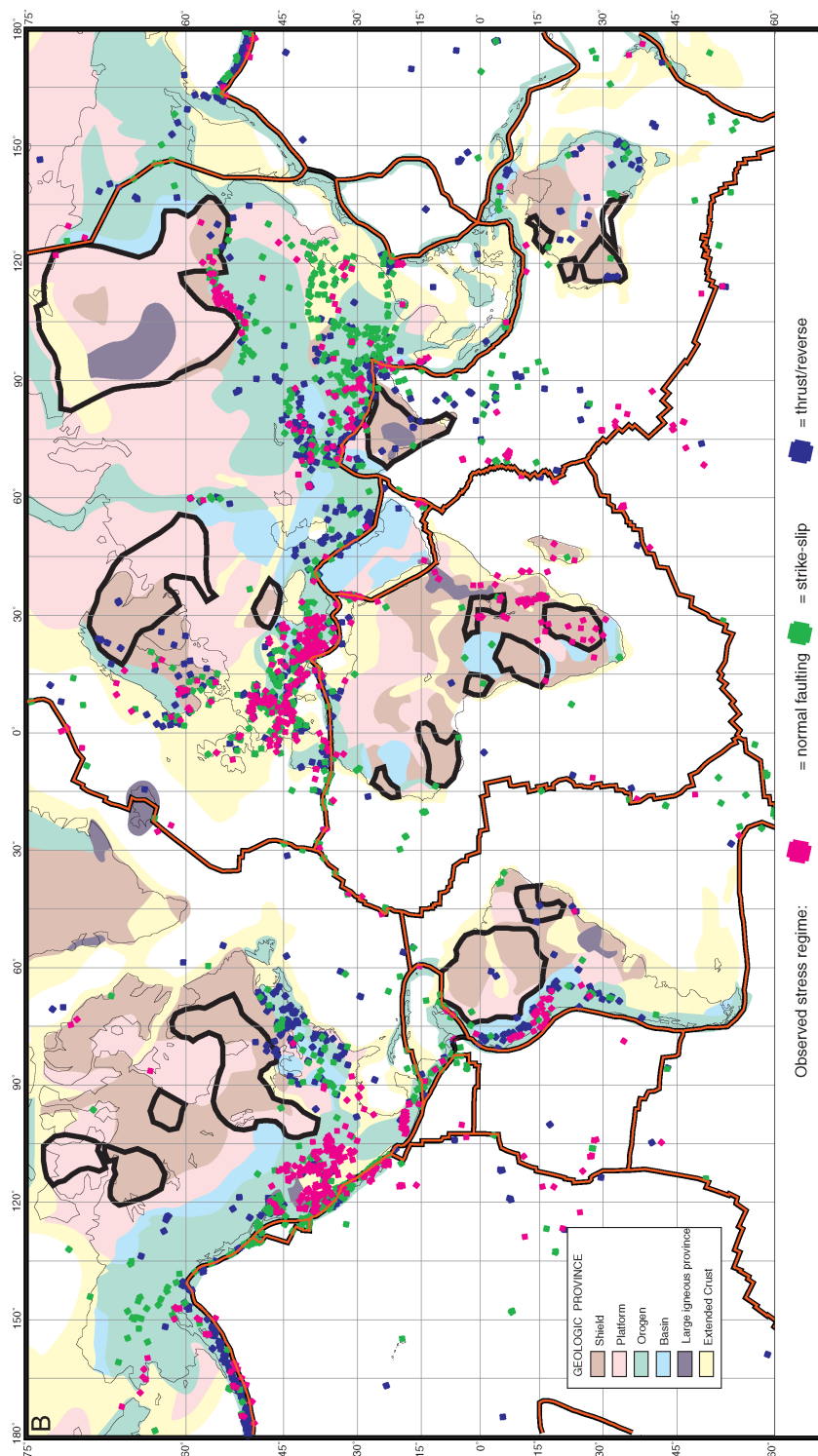


FIG. 10. A. Map of computed potential energy differences relative to the reference asthenosphere geoid. Positive potential energy differences giving rise to deviatoric extensional stresses are shown in red and magenta, weak negative potential energy differences are shown in green, and negative potential energy differences are shown in cyan and blue, and represent the largest deviatoric compression values, implying strong deviatoric compressional stresses. B. Map of observed stress regime data from the World Stress Map database (Zoback, 1992). These represent a subset of the entire database and are those data points with stress regime information, primarily earthquake focal mechanisms and geologic stress indicators. Magenta indicates an extensional stress regime, characterized by normal faulting. Green shows data indicating strike-slip faulting. Blue points represent areas of a strongly compressional stress regime, characterized by thrust or reverse faulting.

red and magenta, weak negative potential energy differences are shown in green to represent a possible strike-slip stress regime, whereas larger negative potential energy differences are shown in cyan and blue, and represent the largest deviatoric compression values, hence implying a thrust/reverse faulting stress regime. These gravitationally derived deviatoric stresses are superimposed on plate driving forces (which are generally compressional within the continents, Richardson et al., 1978; Zoback, 1992) to produce the actual stress state.

There is qualitatively good agreement between the deviatoric stress state predicted from lithosphere buoyancy (Fig. 10A) with the observed stress regime data (Fig. 10B). An extensional stress state is correctly predicted in several regions of active rifting: the Basin and Range province of the western United States, the East African rift system, and the Baikal rift. Western Europe shows a mix of mildly positive and negative potential energy differences, consistent with the observed combined normal/strike-slip stress regime. The potential energy differences computed for the central and eastern United States are scattered, and generally range from mildly to strongly positive, but are consistent with the combination of strike-slip and thrust/reverse faulting observed there. The buoyancy model also predicts large deviatoric compression within the Precambrian shield and platforms, consistent with the thrust and reverse faulting commonly observed in these areas, particularly in the Canadian, Baltic, and Indian shields. Most of the Russian platform and, in particular, the Siberian platform are also computed to be in a state of strong deviatoric compression. However, there is no observed stress regime data (no earthquakes large enough for reliable focal mechanisms) from this region to confirm this. This lack of earthquakes suggests that, although buoyancy-related potential energy differences are strongly compressional, the corresponding lithospheric strength must also be high, thus inhibiting deformation in this region (see Zoback et al., 2002; Thatcher, 2003).

Conclusions

Of all geophysical observations, the topography of the Earth's surface is by far its most accurately known parameter. This fact, together with the large range in elevations, from the deep-sea floor to the highest mountain peaks, has made topographic modeling attractive to Earth scientists for more than

200 years. Our view of the Earth was dramatically refined by plate tectonics theory in the 1960s. A central concept of plate tectonics is a rigid lithosphere floating on a warmer, fluid-like asthenosphere. In this study we reexamine the problem of explaining Earth's topography in terms of "lithospheric buoyancy" using recently available data on global heat flow and the structure of the Earth's crust, as well as by recent insights into the physical properties of the mantle lid (i.e., that part of the uppermost mantle that is part of the lithosphere) from xenolith studies. Buoyancy is determined by the structure and density distribution within the lithosphere. Lateral variations in lithospheric density and thickness give rise to potential energy differences that generate deviatoric stresses. Thus, in addition to explaining topography, our results also help illuminate some of the primary sources of intraplate stress within the lithosphere.

We used global topographic data and a database of more than 1700 crustal structure determinations to evaluate a relatively simple model of lithospheric buoyancy proposed by Lachenbruch and Morgan (1990). The crustal structure compilation indicates that there is no simple relationship between crustal thickness and surface elevation for most continental crust (thicknesses less than 60 km). In fact, major regions of the crust at, or near, sea level (0–200 m elevation) have crustal thicknesses that vary between ~20–50 km. Seismic velocities in the global database were converted layer-by-layer to pressure-corrected densities based on laboratory-determined velocity-density relationships. The results indicate that the mean density of the crust increases regularly with thickness, suggesting that mechanisms of crustal thickening probably involve lower crustal thickening or incorporation of oceanic crust and lithosphere in collisions.

When we attempt to predict topography considering only the crustal contribution to lithospheric buoyancy, we systematically predict elevations that are too high. This implies that the continental crust elevations are generally "pulled down" by a cold lithospheric root that is denser than the asthenosphere on which it floats. To calculate this effect, we must estimate the thickness and density of the mantle lid. To do this, we calculate simple conductive geotherms using measured heat flow values and commonly accepted heat production and conductivity values. These geotherms permit us to estimate the effect of temperature on the density of the mantle lid. The lithospheric thicknesses derived from

the simple buoyancy model of Lachenbruch and Morgan (1990) are in generally good agreement with the 50–300 km thicknesses estimated from seismology, with the important exception of cratonic regions where predicted thicknesses are roughly half those observed seismically. However, if we lower the mean density of the mantle lids beneath Archean cratons by 1% (as previously suggested on the basis of petrologic and geoid studies), we obtain lithospheric thicknesses in those regions of 200–350 km, in accord with seismic estimates.

The negative buoyancy of the mantle lid beneath cratons gives rise to large positive potential energy differences that exert a compressive stress on the overlying crust that is superimposed on the intraplate stresses derived from plate boundary forces. This observation is consistent with the dominance of compressional forces in most continental areas, and specifically the reverse faulting that is often found in cratonic regions. Conversely, positive buoyancy forces (potential energy differences) are found in regions underlain by a thin mantle lid and with high elevation, such as the Basin and Range province of the western United States, the east African rift system, and the Baikal rift. In these areas, unusually low densities in the upper mantle are probably the primary force driving extension in these regions.

The value of our analysis lies not in the precise values calculated for lithospheric thickness (or potential energy differences), but in the trends that can be discerned at both global and regional scale from analysis of very large data sets that sample different crust and tectonic regimes. Our results demonstrate that, globally, surface elevation cannot be simply or reliably predicted from crustal thickness or even the product of crustal thickness and density. Surface topography is suppressed by a cold, dense lithospheric root of variable thickness.

With respect to intraplate stress, our results suggest that calculations of stresses derived from potential energy differences using a simple, constant-thickness model for the mantle lid will underpredict deviatoric compressional stresses in cratonic regions. The reason for this is that the potential energy difference arises from the density moment, that is, the product of density contrast times depth squared. As we have argued that the mantle lids underlying cratons are thicker and less dense than average continental mantle lid, this results in higher deviatoric compressional stresses than are observed in other continental areas.

We conclude that Lachenbruch and Morgan's lithospheric buoyancy model defining the mantle lid simply as a thermal boundary layer works quite well to predict elevation, except in Archean lithosphere, which is less dense than its thermal regime would imply. A 1% reduction of the density of Archean mantle lids, consistent with chemical depletion suggested by a variety of geologic and geophysical data observations, allows the buoyancy model to be applied in those regions and produces lithospheric thicknesses consistent with seismic observations.

Acknowledgments

This paper was presented at a symposium honoring the career and scientific contributions of George A. Thompson held on December 8 and 9, 2001 at Stanford University. George's early work on the interrelationships between gravity, mass distributions, and topography and their effects on tectonics has inspired a whole generation of researchers. We are indebted to him for teaching us the value and power of applying simple physics principles to better understand the processes acting to deform the Earth's crust. We wish to thank Valya Baranova for help with computations and with the heat flow/heat production compilation. We thank David Coblentz, Gary Ernst, Karl Fuchs, Simon Klemperer, Wayne Thatcher, and Mark Zoback for their thoughtful reviews, all of which greatly improved the paper.

REFERENCES

- Airy, G. B., 1855, On the computation of the effect of the attraction of mountain-masses, as disturbing the apparent astronomical latitude of stations of geodetic surveys: *Philosophical Transactions of the Royal Society of London*, v. 145, p. 101–104.
- Anderson, D. L., 1989, *Theory of the Earth*: Malden, MA, Blackwell, 366 p.
- Artemieva, I. M., and Mooney, W. D., 2001, Thermal thickness and evolution of Precambrian lithosphere: A global study: *Journal of Geophysical Research*, v. 106, p. 16,387–16,414.
- Artyushkov, E. V., 1973, Stresses in the lithosphere caused by crustal thickness inhomogeneities: *Journal of Geophysical Research*, v. 78, p. 7675–7708.
- Balling, N., 1995, Heat flow and thermal structure of the lithosphere across the Baltic Shield and northern Tornquist Zone: *Tectonophysics*, v. 244, p. 13–50.
- Boyd, F. R., 1989, Composition and distinction between oceanic and cratonic lithosphere: *Earth and Planetary Science Letters*, v. 96, p. 15–26.

- Boyd, F. R., and McCallister, R. H., 1976, Densities of fertile and sterile garnet peridotites: Geophysical Research Letters, v. 3, p. 509–512.
- Cermak, V., 1993, Lithospheric thermal regimes in Europe: *Physics of Earth and Planetary Interiors*, v. 79, p. 179–199.
- Cermak, V., and Bodri, L., 1995, Three-dimensional deep temperature modeling along the European geotraverse: Tectonophysics, v. 244, p. 1–11.
- Christensen, N. I., and Mooney, W., 1995, Seismic velocity structure and composition of the continental crust: A global view: Journal of Geophysical Research, v. 100, p. 9761–9788.
- Crough, S. T., and Thompson, G. A., 1976, Thermal model of continental lithosphere: Journal of Geophysical Research, v. 81, p. 4857–4862.
- Dahlen, F. A., 1981, Isostasy and the ambient state of stress in the oceanic: Journal of Geophysical Research, v. 86, p. 23–37.
- Davies, G. F., 1979, Thickness and thermal history of continental crust and root zones: Earth and Planetary Science Letters, v. 44, p. 231–238.
- Doin, M. P., Fleitout, L. and McKenzie, D., 1996, Geoid anomalies and the structure of continental and oceanic lithospheres: Journal of Geophysical Research, v. 101, p. 16,119–16,135.
- Dutton, C.E., 1882, *Physics of the Earth's crust*; by the Rev. Osmond Fisher: American Journal of Science, v. 23, p. 283–290.
- Exxon Production Research Company, 1985, *Tectonic map of the world*: American Association of Petroleum Geologists Foundation, Tulsa, OK, 1985.
- Fleitout L., and Froidevaux C., 1982, Tectonics and topography for a lithosphere containing density heterogeneities: Tectonics, v. 1, p. 21–56.
- _____, 1983, Tectonic stresses in the lithosphere: Tectonics, v. 2, p. 315–324.
- Fowler, C. M. R., 1990, *The solid earth*: Cambridge, UK, Cambridge University Press, 472 p.
- Frank, F. C., 1972, Plate tectonics, the analogy with glacier flow and isostasy, in Heard, H. C., ed., *Flow and fracture of rocks*: Washington, DC, American Geophysical Union, Geophysical Monograph Series, v. 16.
- Gardner, G. H. F., Gardner, L. W., and Gregory, A. R., 1974, Formation velocity and density—the diagnostic basis for stratigraphic traps: Geophysics, v. 39, p. 770–780.
- Goodwin, A. M., 1996, *Principles of Precambrian geology*: London, UK, Academic Press, 327 p.
- Grand, S. P., 1994, Mantle shear structure beneath the Americas and surrounding oceans: Journal of Geophysical Research, v. 99, p. 11,591–11,621.
- Haxby, W. F., and Turcotte, D. L., 1978, On isostatic geoid anomalies: Journal of Geophysical Research, v. 83, p. 5473–5478.
- Houseman, G., McKenzie, D., and Molnar, P., 1981, Convective instability of a thickened boundary layer and its relevance for the thermal evolution of continental convergence zones: Journal of Geophysical Research, v. 86, p. 6115–6132.
- James, D. E., Fouch, M. J., VanDecar, J. C., van der Lee, S., and Kaapvaal Seismic Group, 2001, Tectospheric structure beneath southern Africa: Geophysical Research Letters, v. 28, p. 2485–2488.
- James, D. E., and Steinhart, J. S., 1966, Structure beneath the continents: A critical review of explosion studies 1960–1965, in Steinhart, J. S., and Smith, T. J., eds., *The Earth beneath the continents*: Washington, DC, American Geophysical Union, Geophysical Monograph Series, v. 10, p. 293–333.
- Jessop, A. M., Lewis, T. J., Judge, A. S., Taylor, A. E., and Drury, M. J., 1984, *Terrestrial heat flow in Canada*: Tectonophysics, v. 103, p. 239–261.
- Jones, C. H., Sonder, L. J., and Unruh, J. R., 1998, Lithospheric gravitational potential energy and past orogenesis: Implication for conditions of initial Basin and Range and Laramide deformation: Geology, v. 26, p. 639–642.
- Jones, C. H., Unruh, J. R., and Sonder, L. J., 1996, The role of gravitational potential energy in active deformation in the southwestern United States: Nature, v. 381, p. 37–41.
- Jordan, T. H., 1975, The continental tectosphere: Reviews of Geophysics and Space Physics, v. 13, p. 1–12.
- Jordan, T. H., 1978, Composition and development of the continental tectosphere: Nature, v. 274, p. 544–548.
- _____, 1979, Mineralogies, densities and seismic velocities of garnet lherzolites and their geophysical implications, in Boyd, F. R., and Meyer, H. O. A., eds., *The mantle sample: Inclusions in kimberlites and other volcanics*: Proceedings 2nd International Kimberlite Conference, v. 2, p. 1–14.
- _____, 1981, Continents as a chemical boundary layer: Philosophical Transactions of the Royal Society of London, Series A, v. 301, p. 359–373.
- _____, 1988, Structure and formation of the continental tectosphere: Journal of Petrology, special lithosphere issue, p. 11–37.
- Kukkonen, I. T., 1993, Heat flow map of northern and central parts of the Fennoscandian Shield based on geochemical surveys of heat producing elements: Tectonophysics, v. 225, p. 3–13.
- Lachenbruch, A. H., and Morgan, P., 1990, Continental extension, magmatism and elevation; formal relations and rules of thumb: Tectonophysics, v. 174, p. 39–62.
- Lachenbruch, A. H., and Sass, J. H., 1977, Heat flow in the United States and the thermal regime of the crust, in Heacock, J. G., ed., *The Earth's crust*: Washington, DC, American Geophysical Union, Geophysical Monograph Series, v. 20, p. 626–675.
- _____, 1978, Models of an extending lithosphere and heat flow in the Basin and Range province, in Smith, R. B., and Eaton, G. P., eds., *Cenozoic tectonics and*

- regional geophysics of the Western Cordillera: Geological Society of America Memoir 152, p. 209–251.
- Lachenbruch, A. H., Sass, J. H., and Galanis, S. P., Jr., 1985, Heat flow in southernmost California and the origin of the Salton Trough: *Journal of Geophysical Research*, v. 90, p. 6709–6736.
- Lay, T., and Wallace, T. C., 1995, *Modern global seismology*: San Diego, CA, Academic Press, 517 p.
- LeStunff, Y., and Ricard, Y., 1995, Topography and geoid due to lithospheric mass anomalies: *Geophysical Journal International*, v. 122, p. 982–990.
- Lister, C. R., 1975, Gravitational drive on oceanic plates caused by thermal contraction: *Nature*, v. 257, p. 663–665.
- Madsen, J. A., Forsyth, D. W., and Detrick, R. S., 1984, A new isostatic model for the east Pacific Rise crest: *Journal of Geophysical Research*, v. 89, p. 9997–10,015.
- Mareschal, J.-C., 1991, Downward continuation of heat flow density data and thermal regime in eastern Canada: *Tectonophysics*, v. 194, p. 349–356.
- McNutt, M. K., Diament, M., and Kogan, M. G., 1988, Variations of elastic plate thickness at continental thrust belts: *Journal of Geophysical Research*, v. 93, p. 8825–8838.
- Molnar, P., and Tapponier, P., 1978, Active tectonics of Tibet: *Journal of Geophysical Research*, v. 83, p. 5331–5354.
- Mooney, W. D., 1989, Seismic methods for determining earthquake source parameters and lithospheric structure, in Pakiser, L. C. and Mooney, W. D., eds., *Geophysical framework of the continental United States*: Geological Society of America Memoir 172, p. 11–34.
- Mooney, W. D., Laske, G., and Masters, T. G., 1998, CRUST 5.1: A global crustal model at 5°×5°: *Journal of Geophysical Research*, v. 103, p. 727–747.
- Mooney, W. D., Prodehl, C., and Pavlenkova, N., 2002, Seismic velocity structure of the continental lithosphere from controlled source data, in Lee, W. H. K., ed., *International handbook of earthquake and engineering seismology*, v. 81A, p. 887–910.
- Morgan, P., and Gosnold, W. D., 1989, Heat flow and thermal regimes in the continental United States, in Pakiser, L. C., and Mooney, W. D., eds., *Geophysical framework of the continental United States*: Geological Society of America Memoir 172, p. 493–522.
- National Geophysical Data Center, 1988, ETOPO-5, bathymetry/topography data, data announcement 88-MGG-02: Washington, DC, National Oceanic and Atmospheric Administration, U.S. Department of Commerce.
- O'Reilly, S. Y., Griffin, W. L., Djomani, Y. H. P., and Morgan, P., 2001, Are lithospheres forever? Tracking changes in subcontinental lithospheric mantle through time: *GSA Today*, v. 11, p. 4–10.
- Oxburgh, E. R., 1981, Heat flow and differences in lithospheric thickness: *Philosophical Transactions of the Royal Society of London*, series A, v. 301, p. 337–346.
- Panza, G. F., Mueller, S., and Calcagnile, G., 1980, The gross features of the lithosphere-asthenosphere system in Europe from seismic surface waves and body waves: *Pure and Applied Geophysics*, v. 118, p. 1209–1213.
- Parsons, B. E., and Richter, F. M., 1980, A relationship between driving force and geoid anomaly associated with the mid-ocean ridges: *Earth and Planetary Science Letters*, v. 51, p. 445–450.
- Parsons, B. E., and Sclater, J. G., 1977, An analysis of the variation of ocean floor bathymetry and heat flow with age: *Journal of Geophysical Research*, v. 82, 803–827.
- Pinet, C., Jaupart, C., Mareschal, J.-C., Gariépy, C., Bienfait, G., and Lapoigne, R., 1991, Heat flow and structure of the lithosphere in the eastern Canadian Shield: *Journal of Geophysical Research*, v. 96, p. 19,941–19,963.
- Pollack, H. N., 1986, Cratonization and thermal evolution of the mantle: *Earth and Planetary Science Letters*, v. 80, p. 175–182.
- Pollack, H. N., Hurter, S., and Johnson, J. R., 1990, The new global heat flow data compilation: EOS (Transactions of the American Geophysical Union), v. 71, p. 1604.
- Pollack, H. N., Hurter, S., and Johnson, J. R., 1993, Heat flow from the Earth's interior: Analysis of the global data set: *Reviews of Geophysics*, v. 31, 267–280.
- Pratt, J. H., 1855, On the attraction of the Himalaya Mountains, and the elevated regions beyond them, upon the plumb line in India: *Philosophical Transactions of the Royal Society of London*, v. 145, p. 55–100.
- Priestly, K., and Brune, J., 1978, Surface waves and the structure of the Great Basin of Nevada and western Utah: *Journal of Geophysical Research*, v. 83, p. 2265–2272.
- Richardson, R. M., Solomon, S. C., and Sleep, N. H., 1978, Tectonic stress in the plates: *Reviews of Geophysics*, v. 17, p. 981–1019.
- Ritsema, J., and van Heijst, H., 2000, Seismic imaging of structural heterogeneity in Earth's mantle: Evidence for large-scale mantle flow: *Science Progress*, v. 83, p. 243–259.
- Sass, J. H., Blackwell, D. D., Chapman, D. S., Costain, J. K., Decker, E. R., Lawver, L. A., and Swanberg, C. A., 1981, Heat flow from the crust of the United States, in Touloukian, Y. S., Judd, W. R., and Roy, R. F., eds., *Physical properties of rocks and minerals: McGraw-Hill/CINDAS data series on material properties*, v. II-2, p. 503–548.
- Sclater, J. G., Jaupart, C., and Galson, D., 1980, The heat flow through oceanic and continental crust and the heat loss of the Earth: *Reviews of Geophysics and Space Physics*, v. 18, p. 269–311.

- Simons, F. J., Zielhuis, A., and van der Hilst, R. D., 1999, The deep structure of the Australian continent from surface wave tomography, *Lithos*, v. 48, p. 17–43.
- Stevenson, J. M., and Hildenbrand, J. A., 1996, Gravity modeling of a volcanically active site on the East Pacific Rise axis: *Tectonophysics*, v. 254, p. 57–68.
- Thatcher, W., 2003, GPS constraints on the kinematics of continental deformation: *International Geology Review*, v. 45, in press.
- Thompson, G. A., Catchings, R., Goodwin, E., Holbrook, S., Jarchow, C., Mann, C., McCarthy, J., and Okaya, D., 1989, Geophysics of the western Basin and Range province, *in* Pakiser, L. C., and Mooney, W. D., eds., *Geophysical framework of the continental United States: Geological Society of America Memoir 172*, p. 177–203.
- Thompson, G. A., and Talwani, M., *Geology of the crust and mantle of the western United States: Science*, v. 146, p. 1539–1549.
- Turcotte, D. L., Haxby, W. F., and Ockendon, J. R., 1977, Lithospheric instabilities, *in* Talwani, M., and Pitman, W. C., eds., *Island arcs, deep sea trenches and back-arc basins: Washington, DC, American Geophysical Union*, p. 63–69.
- Van der Hilst, R., Kennett, B. L. N., and Shibutani, T., 1998, Upper mantle structure beneath Australia from portable array deployments, *in* Braun, J., Dooley, J., Goleby, B., Van der Hilst, R. D., and Klootwijk, C., eds., *Structure and evolution of the Australian continent: Washington, DC, American Geophysical Union, Geodynamics Series*, p. 39–57.
- Van der Lee, S., and Nolet, G., 1997, Upper mantle S velocity structure of North America: *Journal of Geophysical Research*, v. 102, p. 22,815–22,838.
- Watts, T., 2001, *Flexure of the lithosphere: Cambridge, UK, Cambridge University Press*, 458 p.
- Weiland, C. M., and Macdonald, K. C., 1976, Geophysical study of the East Pacific Rise 15°N 17°N: An unusually robust segment: *Journal of Geophysical Research*, v. 101, p. 20,257–20,273.
- Zoback, M. D., Townend, J., and Grollimund, B., 2002, Steady-state failure equilibrium and deformation of intraplate lithosphere: *International Geology Review*, v. 44, p. 383–401.
- Zoback, M. L., 1992, First- and second-order patterns of stress in the lithosphere: The World Stress Map project: *Journal of Geophysical Research*, v. 97, p. 11703–11728 [see also http://www-wsm.physik.uni-karlsruhe.de/pub/introduction/introduction_frame.html].
-